

Retraction

Retracted: Real-Time Detection of Lower Limb Training Stability Function Based on Smart Wearable Sensors

Journal of Sensors

Received 23 January 2024; Accepted 23 January 2024; Published 24 January 2024

Copyright © 2024 Journal of Sensors. This is an open access article distributed under the Creative Commons Attribution License, which permits unrestricted use, distribution, and reproduction in any medium, provided the original work is properly cited.

This article has been retracted by Hindawi following an investigation undertaken by the publisher [1]. This investigation has uncovered evidence of one or more of the following indicators of systematic manipulation of the publication process:

- (1) Discrepancies in scope
- (2) Discrepancies in the description of the research reported
- (3) Discrepancies between the availability of data and the research described
- (4) Inappropriate citations
- (5) Incoherent, meaningless and/or irrelevant content included in the article
- (6) Manipulated or compromised peer review

The presence of these indicators undermines our confidence in the integrity of the article's content and we cannot, therefore, vouch for its reliability. Please note that this notice is intended solely to alert readers that the content of this article is unreliable. We have not investigated whether authors were aware of or involved in the systematic manipulation of the publication process.

Wiley and Hindawi regrets that the usual quality checks did not identify these issues before publication and have since put additional measures in place to safeguard research integrity.

We wish to credit our own Research Integrity and Research Publishing teams and anonymous and named external researchers and research integrity experts for contributing to this investigation.

The corresponding author, as the representative of all authors, has been given the opportunity to register their agreement or disagreement to this retraction. We have kept a record of any response received.

References

- [1] Y. Zhang, "Real-Time Detection of Lower Limb Training Stability Function Based on Smart Wearable Sensors," *Journal of Sensors*, vol. 2022, Article ID 7503668, 12 pages, 2022.

Research Article

Real-Time Detection of Lower Limb Training Stability Function Based on Smart Wearable Sensors

Ying Zhang 

Department of Physical Education, Henan Institute of Technology, Xinxiang 453003, China

Correspondence should be addressed to Ying Zhang; ying699@hait.edu.cn

Received 26 May 2022; Revised 14 July 2022; Accepted 16 July 2022; Published 30 July 2022

Academic Editor: Gengxin Sun

Copyright © 2022 Ying Zhang. This is an open access article distributed under the Creative Commons Attribution License, which permits unrestricted use, distribution, and reproduction in any medium, provided the original work is properly cited.

The research of smart wearable sensors in limb training has great application significance. In the face of real-time detection requirements, this paper proposes a hardware solution for the stability function of lower limb training based on the theory of intelligent wearable sensors. For the specific implementation circuit of the device, considering the reliability of the system, the system implements antijamming design for the hardware circuit from three aspects: adding decoupling capacitors, optimizing layout and wiring, and rationally grounding the hardware circuit, and performs moving average filtering on the collected sensor data to remove noise, which solves the problem of sensor data precision issues. During the simulation process, by analyzing the changes of acceleration, angular velocity, and attitude angle under different lower limb training activities and different wearing positions, the characteristics of stability combined acceleration, combined angular velocity, and attitude angle were constructed, and the stability mean, variance, and attitude angle were extracted. The experimental results show that the extracted 57 feature dimensions are first reduced to 21 dimensions by the principal component analysis algorithm, and then, the optimal feature subset is selected by the encapsulation method, and the dimension is reduced to 9. The proposed multifeature fusion algorithm has higher accuracy, and the maximum has increased by 6.5%, effectively improving the accuracy of the lower limb training stability function detection algorithm.

1. Introduction

The advancement of wearable sensor technology has brought great convenience to human daily life, and these rapidly developing sensor technologies have shown strong advantages in sports assistance, medical care, and security monitoring [1]. Especially in the past few years, electronic technology and small sensor systems have developed extremely rapidly [2], especially now that almost everyone has integrated microsensor systems in smart products, which makes the research based on inertial sensors very important [3]. At present, there are more and more researches on human lower limb training and recognition technology [4]. The development of human lower limb training and recognition based on video technology is relatively early, but it will be affected by light or occluders [5], and it has small size and low power consumption for inertial sensors with advantages such as cost and easy portability highlight their advantages, making the recognition technology of human lower limbs based on iner-

tial sensors a hot research topic [6]. Therefore, combining human lower limb training recognition based on wearable inertial sensors with people's daily life can effectively promote people's health management and abnormal lower limb training detection [7].

At present, there has been a great breakthrough in the research on human lower limb training recognition based on multiple inertial sensors. Multiple sensors can collect information about human motion recognition relatively comprehensively [8–11], but it will increase the user's experience burden and make the user more comfortable. It will also increase the amount of calculation during data analysis. The current research tends to use fewer sensors to obtain more comprehensive lower extremity training information, so this paper uses a single inertial sensor to collect data [12]. At present, the application of classifiers has been more and more mature, but there are still some technical problems to be solved in the signal processing stage, so the technology of feature extraction and selection still needs to be deeply

explored, how to select suitable features and how many dimensions to select [13], which feature selection method is used, can make the calculation efficiency high, the calculation complexity low, and the recognition accuracy high [14–17]. Therefore, this paper designs a single sensor-based human lower limb training and recognition algorithm and mainly focuses on the extraction and selection of features.

In terms of software design, this paper divides the software system into two parts: the lower computer and the upper computer. Among them, the lower computer part mainly designs the five modules of rehabilitation training, data acquisition, data storage, communication, and clock, and explains it through the flow chart; the upper computer part mainly focuses on the training plan and related parameter download, real-time pressure curve display, and training record generation. These three functions are designed. From this, the software core of the whole system and its working process is expounded. First, the rotation angle information is introduced on the basis of traditional statistical features and frequency features, which is more conducive to identifying the changes of actions in three-dimensional space. Secondly, the process of feature extraction plays a key role in the entire human lower limb training and recognition algorithm. The number of features is too small to completely contain all the action information. Too many features will occupy too much memory, increase the computational complexity, and reduce the computational complexity. Therefore, in view of the problem of high feature dimension in the feature extraction process, this paper designs and studies a combined dimension reduction method, which combines principal component analysis and feature subset selection algorithm to effectively reduce the feature dimension. Two classification algorithms, hidden Markov model in supervised learning and fuzzy C-means clustering in unsupervised learning, are selected as the best choice. The multifeature fusion algorithm is verified and explained, and the fuzzy C-means clustering algorithm is currently more used in image processing, and it is a new application in the recognition of sensor data.

2. Related Work

A flexible wearable heart rate/pulse sensor refers to a flexible wearable monitoring and sensing device that converts heart rate and pulse signals into electrical signals. As the core sensing component of wearable health monitoring equipment, the flexible wearable heart rate sensor can realize real-time monitoring of healthy vital signs by wearing it on the human body, providing new solutions and technical means for health prediagnosis and personalized home monitoring [18]. At present, in the field of professional clinical applications, the commonly used sensors for measuring heart rate and lower extremity training mainly use electrical, optical, and strain transmission in principle sense and other technical means and methods to achieve.

With the development of electronic science technology and material technology, various wearable sensors with small size, low power consumption, and intelligence have received extensive attention and in-depth research from all

walks of life, and have become one of the research hotspots in recent years, and have achieved certain research progress and research results. Greco et al. [19] fabricated a wearable ECG sensor system through a serpentine mesh copper electrode in the form of a Band-Aid, which possesses the stretchability and flexibility required by wearable devices. Zhou et al. [20] realized the acquisition of ECG lower limb training signals by printing two gold electrodes on a polyimide screen. The acquisition circuit hardware system and sensors are integrated into the flexible PCB to form a wearable flexible lower limb training monitoring system. Chen et al. [21] integrated the ECG acquisition electrode and the flexible piezoresistive sensor into one, and made a wristband-type sensor system, and the sensor system can realize the fusion of pulse pressure signal and ECG signal, thereby realizing accurate real-time blood pressure.

To sum up, in recent years, the development of flexible wearable sensors has been very rapid, and they have broad application prospects in the fields of intelligent electronic perception, intelligent robots, clinical decision-aided diagnosis, chronic disease health management, sports health care, environmental monitoring, aerospace, and other fields. Wu et al. [22] used support vector machine to analyze the foot force curve of athletes. The study automatically divides the curve into five stages to build the classifier. Although the classification effect is satisfactory, it is to single based on the information of a six-dimensional torque sensor. The application of neural network classifiers to EMG signals only has a good effect on the action recognition of upper limbs, because the EMG signals of changes in upper limb movements are easier to collect and identify, and the EMG signal processing of lower limb movements is not ideal. For example, the neural networks and Markov models are used to process EMG signals, which can identify movements such as upper limb reversal and bending. Although the research in the field of flexible heart rate and pulse sensors has achieved certain results, there is still room for continued research and exploration in the selection of flexible materials and the preparation of sensors, and there is still a certain amount of research achievements into clinical applications [23].

3. Real-Time Detection Model Construction of Lower Limb Training Stability Function

3.1. Frequency Collection of Smart Wearable Sensors. The smart wearable sensing system uses Anxinke A9G module for positioning, which supports three positioning methods: GPS, BDS (BeiDou Navigation Satellite System), and base station positioning. Base station positioning is the position coordinates obtained by calculating the difference value of base station signals, which is greatly affected by the environment. The error in remote areas can reach 1000-2000 meters, and the positioning error is relatively large. However, GPS and BDS positioning are more accurate, as long as four satellite signals are received, precise positioning can be carried out, and the positioning error is within 5-10 meters.

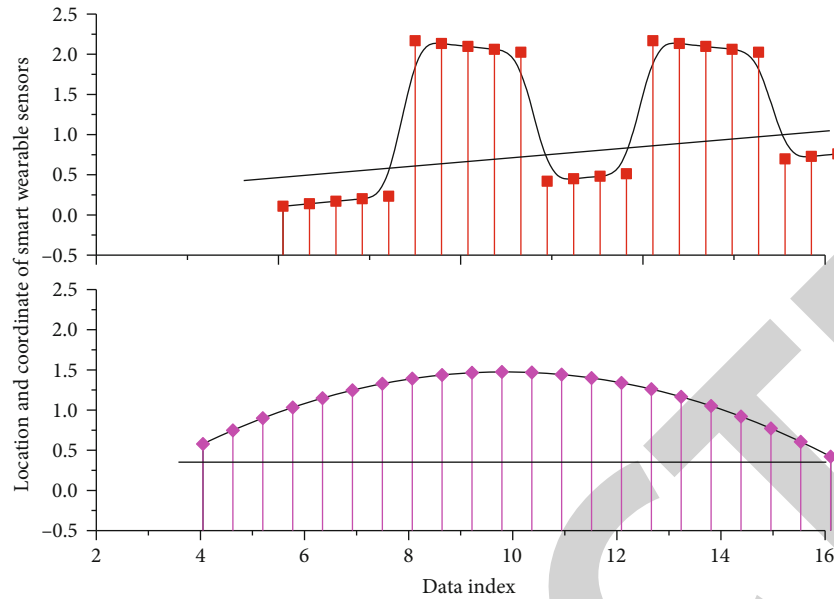


FIGURE 1: Distribution of position coordinates of smart wearable sensors.

The applications are quite different. The wrapper uses the accuracy and recognition rate of the classifier as the criteria for judging whether the feature subset can be applied. The deviation is small, but it is not suitable for scenarios with large feature dimensions. There are two main development methods for A9G modules, namely, AT command development and firmware development. AT command development refers to sending corresponding GPRS/GPS commands through an external controller using a serial port to complete positioning and information transmission; firmware development refers to downloading. The corresponding program is put into the module, and the development directly on the module does not require an external controller. Considering the difficulty of firmware development and the problem of system acquisition and classification, the system uses the serial port on the core board to send AT commands to control the A9G module to transmit and locate the data in Figure 1.

Compared with the results of wearing on the waist position, it can be seen that the recognition rate of wearing on the right front hip is lower than that of wearing on the waist and back. For the feature selection algorithm proposed in this chapter, the waist is the best place to place the sensor. The experimental verification method is also the ten-fold cross-validation method. All the data are divided into ten groups, and the data of one group is selected as the test set in turn, and the data of the remaining 9 groups is the training set. The average accuracy in Table 1 is 91.3%, and the diagonal value is an average accuracy result.

The DSAD data set contains 8 volunteer data. Each time, one volunteer data is taken for testing, and the remaining volunteer data is used for training to obtain 8 sets of test data. Each set of test data contains 1,140 action sequences. The set contains 7980 action sequences. Compared with the traditional simple voting method, the results are as shown. Finally, the average of the 8 groups of results is aver-

TABLE 1: Description of smart wearable sensors.

Training number	Volunteer data	Diagonal value	Confusion matrix	Average accuracy
1	44.034	22.864	1.341	0.822
2	41.108	24.268	1.305	0.853
3	37.677	25.915	1.269	0.884
4	34.401	27.487	1.233	0.915
5	32.100	28.592	1.197	0.946
6	31.494	28.883	1.161	0.977
7	32.937	28.190	1.125	1.008

aged, and the average recognition rate of the fusion results using the simple voting method is 82.4%. The multitask result fusion proposed in the paper is used. The average recognition rate of the method can reach 89.7%, which is about 7% higher, and the corresponding confusion matrix is shown in the paper. The main reason is that the periodicity of these two actions is not strong, and the selected 24 sampling points are not enough to fully represent the action, which highlights some problems in the selection of fixed windows to a certain extent. The rate is lower than that of the WARD data set, but the actions in both data sets are compared, such as standing, sitting, and going up and down stairs. Through the Bluetooth connection of the sensor, the computer transmits the data of normal pedestrians walking indoors in real time, and saves it. Among them, except that the dimensions of the features are different, the rest of the settings are exactly the same.

3.2. Mathematical Analysis of Lower Limb Training Stability.

The exercise state of lower body training only considers several common movements in daily life, not the movements during vigorous exercise. The experimental materials and

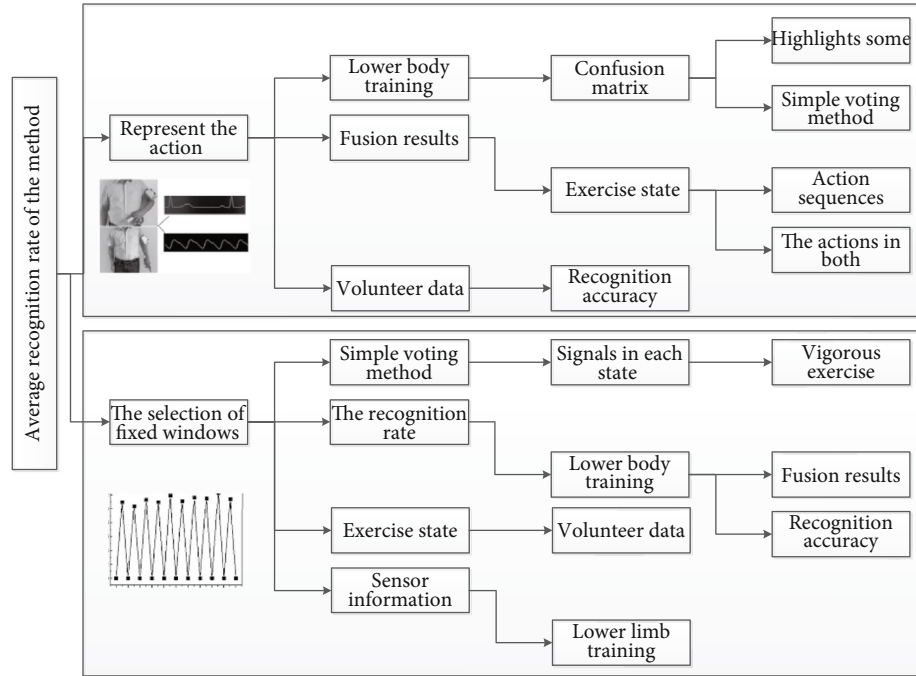


FIGURE 2: Intelligent wearable sensor monitoring system.

test environment were the same as those of the static ECG test. The subjects performed three movements of standing, swinging, squatting, and rotating, and recorded the ECG signals in each state, and 9 seconds of data is recorded and stored. Different sensor wearing positions will affect the recognition accuracy. In order to verify the differences caused by different sensor wearing positions, this paper uses the public USC-HAD data set (ACM, Pittsburgh, PA, USA) for classification and recognition. The acquisition device is an integrated sensing platform MotionNode, which captures human activity signals and constructs a data set. The researcher places the sensor on the right front hip.

The real-time wearable lower limb training monitoring system mainly includes the three-layer structure shown in Figure 2. The first layer is the sensing layer, including flexible dry electrodes, lower limb training acquisition units, signal storage, and transmission units. A bigger challenge for deploying an effective and reliable human action recognition system is how to compact a multisensor architecture, find a balance between recognition accuracy and deployment cost, and achieve better recognition results with as little sensor deployment cost as possible.

The second layer is the network layer, including wireless communication module, big data storage and calling module, and cloud computing module. Figure 3 transmits the received lower limb training signal to the cloud through WIFI network or 4G/5G network via TCP/IP network protocol. The platform saves and manages structured data, and the cloud computing module calls the large-scale lower limb training data for automatic lower limb training signal processing and diagnosis, and feeds back the analysis results and abnormal heartbeat warnings to the application layer. The third layer is the application layer, including real-time analysis module and post-processing module.

3.3. Real-Time Detection Data Segmentation. Before the real-time test, the subjects sit still for 5 minutes and keep breathing evenly and feel calm. The ECG signal acquisition adopts the connection method of the chest leads. The self-made lower limb training acquisition board is used for measurement. The distance between the center points of the positive and negative electrodes is fixed as 8-9 cm apart. The room temperature is about 25°C, and the relative humidity is 65% ± 2%. After data preprocessing, the acceleration value, angular velocity value, and magnetic field value are directly analyzed using the corresponding time domain and frequency domain features to form a feature data set, and then use the feature data set to train the algorithm model, which may lead to the comparison of the accuracy of the algorithm model. Therefore, this paper selects features such as combined acceleration, combined angular velocity and attitude angle, and uses these feature data for subsequent algorithm model training and testing. Cross-user behavior recognition is performed on the 60-dimensional features extracted from the courier data set, and the improved cosine-weighted CORAL algorithm is compared with several different unsupervised domain adaptation methods and traditional CORAL.

$$T(x, y, u|x = 1, 2, 3, \dots, n) = \begin{bmatrix} u(x-3, y-1) \\ u(x-2, y) \\ u(x-1, y+1) \end{bmatrix}, \quad (1)$$

$$lameda(a, b) \leftrightarrow \begin{cases} [u(a, \text{for}, \{a = a - 1, 0\})] \\ [u(b, \text{for}, \{b = 1, 0\})] \end{cases}$$

After obtaining the 12-lead NVC values for all MI models, the NVCs were mapped to a 3×3 color matrix,

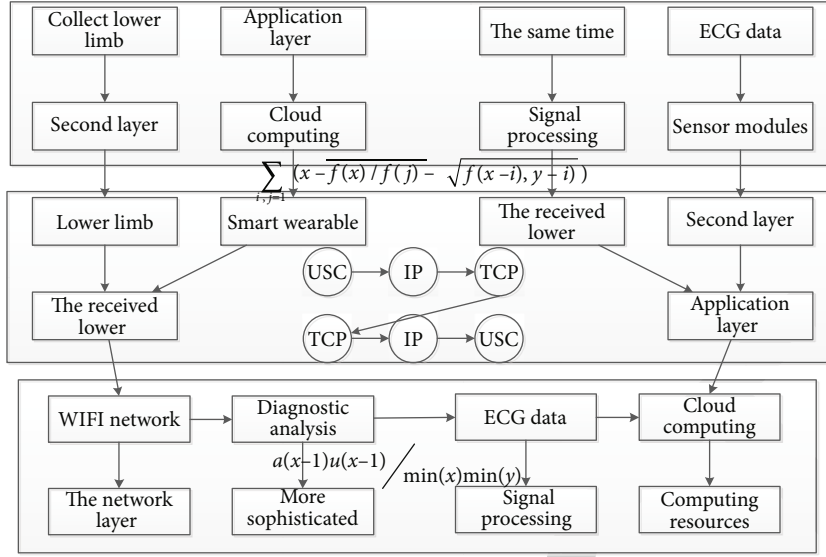


FIGURE 3: Distribution of smart wearable sensor modules.

representing 3 sizes and 3 positions. Each color is displayed with different grayscale values between white and black, depending on the value of the NVC, to indicate the degree to which different MIs affect the ECG morphology in a particular lead.

$$\begin{cases} \sum \text{trace}(f(a), f(b)) - v(a)v(b) < 1 \\ \sum_{m,n=1} 1 - \frac{1-a-b}{f(a)f(b) - v(a)v(b)} > 1 \end{cases}, \quad (2)$$

$$\int g(t(x) - t(j)) - \int g\left(\frac{i(x)}{j(t)}\right) dt - \int \left(\frac{j(x)}{i(t)}\right) - 1 = 0.$$

The rule-based long-term lower limb training detection algorithm includes four modules. The first module is preprocessing and feature detection on the 24-h signal. The second module is to extract the heartbeat template based on the results of preprocessing and feature detection, construct the templates of primary and secondary heartbeats, and determine the template type. The third module is rhythm calculation, which finds heart beats that satisfy the rules of lower limb training rhythm information. Finally, each beat is classified according to the constructed beat template and the rhythm information of the beat.

$$X(i, j) = \sum_{i,j=1} \overline{f(i)/f(j)} - \frac{u(i)}{u(j)} - \sum_{i,j=1} \overline{f(i) - 1/f(j)} - \frac{u(i) - 1/u(j)}{1 - i},$$

$$\begin{cases} \sum_{i,j=1} \overline{f(x)/f(j)} - t(x, j) < 1 \\ \sum_{i,j=1} \frac{\sqrt{f(x) - t(x, j)}}{f(y)} = 0 \end{cases}. \quad (3)$$

The location of each QRS complex in these data and its type (N, PAC, or PVC) was separately annotated by two

independent cardiologists. If the annotations by the two experts are inconsistent, a third cardiologist is referred to arbitration. Then, we randomly select a lead signal from the original 12-lead data to form the training set data, which is used to train the algorithm rules.

$$f(i, j) = \begin{cases} \sum_{i,j=1} \left(\frac{f^{t-i}(i-x)}{(1-j-y)} \right) \\ \sum_{i,j=1} \left(\frac{f^{t-i}(i)}{f^{t-j}(j-y)} \right) \end{cases}, \quad (4)$$

$$\sum_{i,j=1} \left(\frac{u^{t-i}(i)}{u^{t-j}(j)} \right) - \left(\frac{u(i)}{u(j)} \right) \in \{i, j = 1, 2, 3, \dots, n^2 - 1\}.$$

The Xsens Xbus Master inertial motion capture device is used to acquire the data set. Multiple motion capture systems (MTx) are connected in series through one or more Xbuses. The MTx corresponds to the sensor node and can provide unbiased 3D positioning and kinematics data. Xbus Master connects to PC via cable or wireless for data transfer.

$$\begin{cases} \min \left\{ \frac{1 - u^{t-i}(i)}{u^{t-j}(j)} \right\} > 1 \\ \max \left\{ \frac{u^{t-i}(i)}{u^{t-j}(j)}, u^{t-i}(i), u^{t-j}(j) \right\} < 1 \end{cases},$$

$$jogger(i, x) = \sum_{i,j=1} u^{t-i}(i) / \sum |1 - u^{t-j}(x)| - \sum_{i,j} |1 - u(i)| / |1 - u(x)|. \quad (5)$$

5 sensor nodes at a time obtain a $5 \times 3 \times 3 = 45$ -dimensional time series data, where 5 represents 5 sensor nodes, the first 3 represents the 3 different sensor types in each sensor node, and the second 3 represents three sample values for each sensor type. The sampling time of each action sequence

is 5 s; that is, an action sequence is a 125×45 -dimensional motion vector.

$$\begin{aligned} & \frac{1}{i-j} \sum_{i,j=1} \left(x - \frac{f(x)/f(j)}{f(j)} - \sqrt{f(x-i, y-i)} \right) \\ & - \sum_{i,j=1} \frac{\sqrt{f(x-y) - f(x+y)}}{\sqrt{f(x)f(y)}} = 0, \quad (6) \\ & a(x)u(x) + a(x-1)u(x-1) + a(x-2)u(x-2) \\ & + \dots + a(x-i)u(x-i) \subseteq AU(x). \end{aligned}$$

Sparse representation means that in a large enough training sample space, for a class of objects, it can be roughly linearly represented by the same sample subspace in the training sample, so when the object is represented by the entire sample space, its representation coefficients are sparse.

$$\begin{aligned} & \sum_x^{x-i} a(x) \sqrt{u(x=1, 2, 3, \dots, n)} \\ & + a(x-1) \sqrt{u(x-1=1, 2, 3, \dots, n)} + x = 1, \quad (7) \\ & z(x, y) = \begin{cases} \frac{a(x-1)u(x-1)}{\min(x) \min(y)} \\ \frac{a(x-i)u(x-i)}{\min(x-i) \min(y-i)} \end{cases} \end{aligned}$$

It is verified that the motion data acquired by the sensor is sparse, and the acquisition of lower limb training data is achieved through multiple sensor nodes. Using the sparse expression classification method, the problem to be solved can be transformed into a multiple linear regression model.

The residual dictionary is manually divided into two categories: One is consistent with the real category, and the other is other category actions that are different from the real category. Since the recognition ability of the same task for different actions is different, the paper establishes a training set according to the category. Since the same task has different distinguishing abilities for different lower limb training actions, the paper establishes a residual training set according to the lower limb training categories. In order to ensure the comparability of multiple residual fusion values obtained by one lower limb training in one test, the paper normalizes the residual weight coefficients of each task.

4. Application and Analysis of Real-Time Detection Model for Lower Limb Training Stability Function

4.1. Smart Wearable Sensor Data Sampling. In the process of lower limb training data collection, the frequency of collection also plays a crucial role. Too small or too large frequency will have an impact on data processing and recognition accuracy. The higher the frequency, the more lower limb training information can be displayed. However, it will increase the power consumption during processing. If

the frequency is too low, it is impossible to obtain complete lower limb training feature information. By reviewing a large number of literatures, the frequency used by the researchers is mostly between 20 Hz and 150 Hz. Considering various factors, this paper can set the sampling frequency to 100 Hz. The DSAD data set is tested with 10-fold cross-validation method, the parameters are set to default values, and the behavior recognition rates before and after the extraction of associated features are compared. Under the three methods, the misrecognition rate of lower limb training with associated features is slightly lower than that without associated features, and the average difference is about 1%.

One of the cores of the multilevel decision-making behavior recognition method is that the data of each sensor is calculated independently, which has achieved the purpose of low coupling, so it is necessary to classify the data according to the label number which are different subdata sets. The confusion matrix is as shown, and the value corresponds to the recognition percentage. The results in Figure 4 fully demonstrate the effectiveness of the proposed features.

The system software is developed collaboratively using C and Python languages. The Python language mainly trains, optimizes, and saves the wearing position recognition algorithm and the lower limb training detection algorithm of the lower limb training detection device in the PyCharm integrated environment under the Windows platform; the C language mainly develops the functions of data acquisition and alarm information sending on the Linux platform. The software of the system mainly includes initialization, data acquisition, wearing position recognition algorithm, lower limb training detection algorithm, positioning method and alarm sending. The development process is to initialize the system first, including the initialization of I2C, UART, jy901b, and GPRS/GPS modules, then perform data acquisition, call functions in python for data preprocessing and feature selection, and call the trained system algorithm for lower limb training detection.

It can be seen from the figure that for this article the proposed multifeature fusion algorithm, using the unsupervised FCM algorithm, has a significantly higher recognition rate than the HMM algorithm in supervised learning, which strongly proves the advantage of the FCM algorithm based on wearable inertial sensors. If there is no lower extremity training, continue to collect the data in Figure 5 for analysis and judgment.

It can be seen that the Se identified by the original AlexNet model for N, PAC, and PVC is 83.66%, 73.16%, and 77.66%; P+ is 85.73%, 70.09%, and 78.58%; Acc is 78.38%; and the identified F1 measure reaches 91%. The overall F1 measure was 78.13%. After our improvement on the original AlexNet model, the Se of N, PAC, and PVC are 88.74%, 78.95%, and 86.28%; P+ are 94.7%, 76.79%, and 83.44%, respectively; Acc is 85%; the identified F1 measure reaches 91.63%, 77.86%, and 84.83%; and the overall F1 measure is 84.77%, which shows that our improvement of the model is of great help in improving the recognition accuracy of the lower limb training of the two-dimensional model. CPSC2018 provided participants with 9 types of 12-lead clinical lower extremity training data (including normal

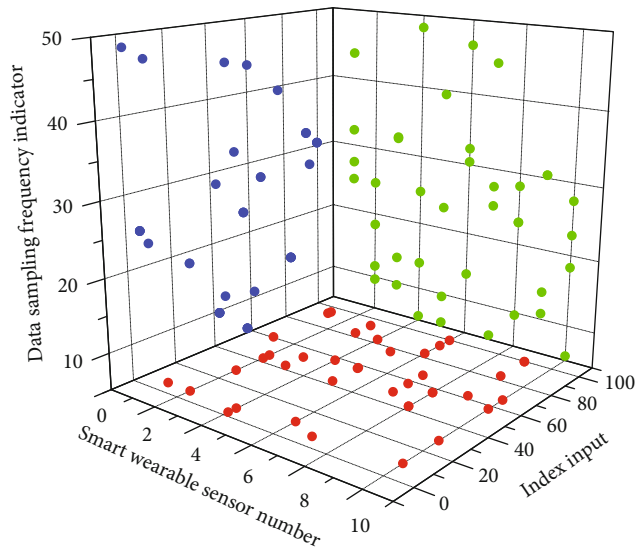


FIGURE 4: Data sampling frequency distribution of smart wearable sensors.

and 8 abnormal types) marked by doctors. The sampling frequency of the data was 500 Hz, and the data length ranged from a few seconds to dozens of seconds. Among them, the numbers of N, PAC, and PVC signals were 918, 556, and 672, respectively, and the time lengths were 15.43 ± 7.61 s, 19.46 ± 12.36 s, and 20.21 ± 12.85 s, respectively.

4.2. Simulation Realization of Lower Limb Training Stability.

The hardware system platform of the smart wearable sensor is designed. The hardware part mainly includes data acquisition module, processor module, power supply module, GPRS/GPS module, and alarm module, and the algorithm performance test of the hardware system platform is carried out, and it is found that the lower limb training detection is compared. The device's wearing position recognition algorithm and the lower limb training detection algorithm have high accuracy. The overall schematic diagram of the lower limb training detection equipment mainly includes the slot of the core board, the A9G module, the GSM (Global System for Mobile Communications)/GPS antenna, the SIM card module, the jy901b module, the buzzer module, and the button module, network interface, and power boost module. The A9G module, GSM/GPS antenna, and SIM card module constitute the overall GPRS/GPS transmission and positioning module. For the convenience of program development, a network interface is designed for program download.

In order to further verify the proposed algorithm, the paper also did a lot of experiments on the DSAD database. In the DSAD data set, the number of lower limb training in Figure 6 is $N = 19$. The number of sensor nodes L is 5. But it contains more abundant sensor information (each sensor node contains three-axis accelerometer, three-axis gyroscope, and three-axis magnetometer), namely, K is 9. The sensor information is selected with the duration of 24 sampling points as the window size to form a training set and a test set, that is, $h = 24$. The resulting quadruple is (5, 19, 9). The tag is a sensor tag based on a positioning system,

and the collected data reflects the tag. For the location information at each moment, the sampling frequency is generally set to 10 Hz. After the collection is completed, the sorting of the data is the most important step. The jy901b module collects the acceleration value, angular velocity value, magnetic field value, and attitude angle value of the human body and transmits the data to the core board through the I2C protocol. The core board parses the data according to the data format and range of the jy901b sensor (acceleration value ± 16 g, angular velocity value $\pm 2000^\circ/\text{s}$, and attitude angle $\pm 180^\circ$) for analysis and processing.

For the identification in Figure 7, both PAC and PVC had a maximum error of 100%, which occurred in volunteers 2, 9, 10, and 7, respectively. Among them, volunteer No. 2 was a patient with atrial fibrillation, and the rhythm rules in the algorithm identified the data segment of atrial fibrillation as PAC, resulting in a high false detection rate of PAC. The PAC errors of No. 9 and No. 10 volunteers are both due to the detected number being twice the number reported by Holter, but from the actual number of detections, the numbers detected by the algorithm are all within the acceptable range. We selected 40 data excluding pacing signals as the algorithm's test data. Most of the data in the MIT-BIH-AR database were a combination of modified limb II lead data (45 data with MLI lead signal) and prethoracic lead data (40 data with V1 lead signal). In this chapter, we define these two lead signals as lead A and lead B signals and evaluate the performance of our algorithm on both leads separately. The sampling frequency of these data is 360 Hz.

4.3. Real-Time Detection Feature Extraction.

The basic steps of the real-time detection feature algorithm are as follows: (1) First, use the 10-fold cross-validation method to divide the collected data into the data set. (2) After preprocessing the classified data signal, select the dimension-reduced data signal. Several features such as time domain and frequency domain are used to represent the characteristic information of pedestrian actions. (3) 8 kinds of actions such as standing still, walking forward, running forward, turning left, turning right, going upstairs, going downstairs, and bending over are recognized. The optimal feature subset can reduce the dimension more effectively. Currently, the most used methods mainly include filter and wrapper.

The FCM algorithm does not need the parameters of the training model, but only needs to calculate the distance between the test sample and each cluster center, which has the advantage of simplicity and practicality. Traditional machine learning needs to traverse all the data. If there are too many training samples, it will consume a lot of time. The wrapper uses the accuracy and recognition rate of the classifier as the criteria for judging whether the feature subset can be applied. The deviation is small, but it is not suitable for scenarios with large feature dimensions. Therefore, it can be combined with PCA to effectively select Table 2 for feature subset.

The collected signals are stored locally. After the processing module is connected to the smartphone, the data is transmitted to the mobile phone through Bluetooth for real-time display and is uploaded to the cloud database.

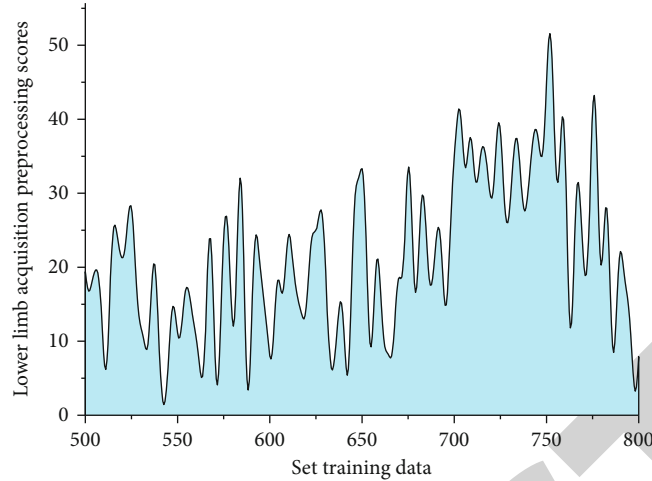


FIGURE 5: Preprocessing of lower limb training data acquisition.

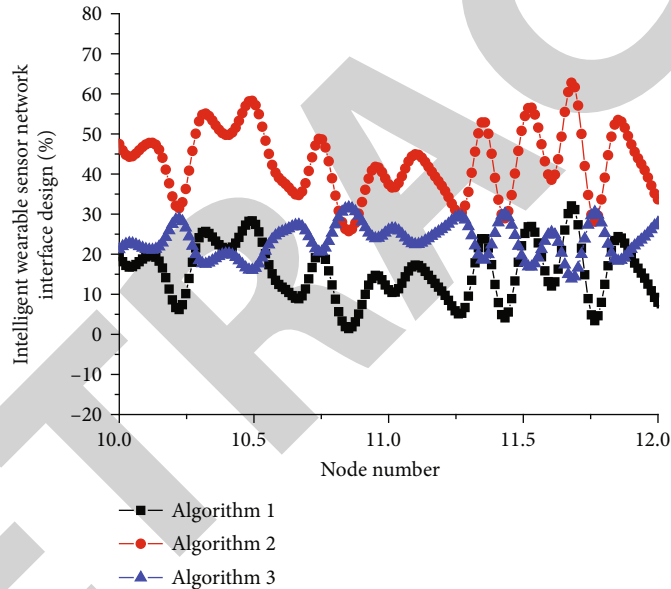


FIGURE 6: Design of smart wearable sensor network interface.

Twenty volunteers between the ages of 26 and 65 with a history of lower body training participated in the study, each collecting 30 minutes of data. The data was split into 10-second segments with no overlap, and the quality of each segment was manually checked. Each R-wave location and its type (N, PAC, or PVC) in these 10-second data segments was annotated by two independent experts and arbitrated by a third expert. The data shows the change of the lower limb training misrecognition rate and execution time in the process of increasing the number of tasks from 1 to 6.

When the number of lower limb training increases to 6, the execution time begins to increase. It can be seen that multitasking can improve the execution time of lower limb training recognition to a certain extent, but too many tasks will have a negative impact. This is mainly when the number of tasks is much larger than the number of system cores, and the task switching time overhead is increased during the task

execution process. Therefore, an appropriate number of tasks can be selected according to the processing system.

It can be seen from Figure 8 that the average error between the total heartbeats detected by the algorithm and the total heartbeats reported by Holter is $5.21 \pm 2.09\%$, and the average error of the normal heartbeats detected by the two is $4.66 \pm 1.92\%$. On PAC and PVC identification, the mean errors between our algorithm and Holter's report were $47.1 \pm 40.84\%$ and $24.21 \pm 32.62\%$, respectively. This experiment is aimed at continuous action time series, using the extracted feature dimension, which can be effectively identified in the classifier based on the HMM model. For the 8 lower limb movements collected by myself in this study, the highest recognition rate can reach 95%, and the average recognition rate is 92.5%. When evaluating the performance of a human body's daily lower limb training recognition model, not only the recognition accuracy, but also the

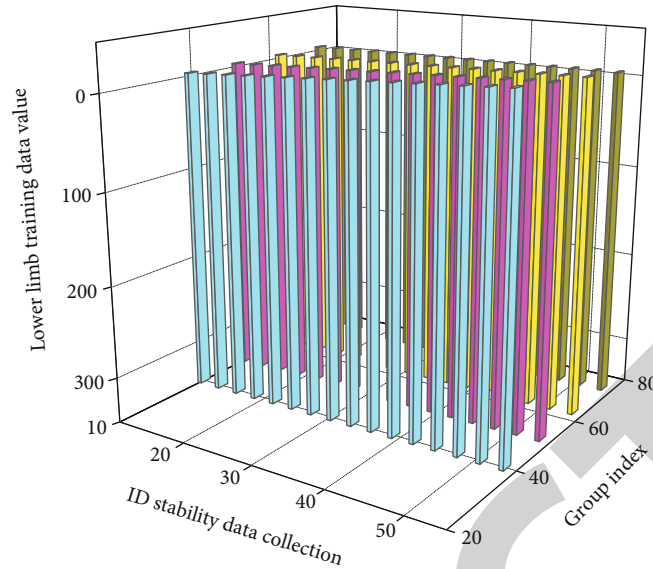


FIGURE 7: Data collection of lower limb training stability.

TABLE 2: Real-time detection feature algorithm.

Real-time detection function	Feature algorithm test
<code>#include<iostream></code>	Optimal feature subset
<code>#include<vector></code>	Basic steps
<code>Vector<string> split(string &s,char mode){</code>	Turning right
<code>Vector<string> res;</code>	Walking forward
<code>While(s.size() >0){</code>	Going upstairs
<code>Int index = s.find(mode);</code>	Running forward
<code>If(index != -1){</code>	Going downstairs
<code>In.getline(line,512,'\n');</code>	Information of pedestrian actions
<code>String src = string(line);</code>	Turning left
<code>Lines.push_back(split(src,','));</code>	Internal feature measurement

efficiency of the algorithm in the model and the recognition speed should be considered. The recognition rate of most actions can reach more than 90%. Although the accuracy rate is slightly lower than that of the HMM model, there are also advantages. For example, the computational complexity of the KNN algorithm is low, but it lacks the advantages of timing signals.

4.4. Example Application and Analysis. The front of the smart wearable sensor is the Allwinner H5 core board, power module, Anxinke A9G module, and jy901b module; the reverse is the SIM card holder. The antennas in the figure include GPS antennas and GSM antennas, which provide guarantees for information transmission and positioning. This paper first judges the wearing position of the wearable device according to the Softmax algorithm and then uses the feature selection and KNN algorithm to judge the lower limb training. Therefore, it is necessary to wear the fall detection device on the waist, chest, wrist, and ankle for experimental test analysis. Correlation features are obtained

by fusing multiple sensor data. When lower limb training occurs, there are differences between sensor data located at different positions of the body, and for different actions, this difference is also different; that is, the correlation between the same sensor nodes corresponding to different actions is not the same. It can be seen that there are differences between the data of each sensor node.

When evaluating the performance of a human daily behavior recognition model, not only the accuracy of recognition, but also the efficiency of the algorithm in the model, the speed of recognition, should be considered. The associated features are extracted from the existing data, no additional data transmission is required, and the energy consumption problem of additional data transmission is avoided.

The accuracy rate of the human lower limb training recognition algorithm based on HMM design is mostly above 90%, and the accuracy rate of Figure 9 is guaranteed. However, the data set collected in this paper is limited. In view of the differences between humans, it is necessary to verify

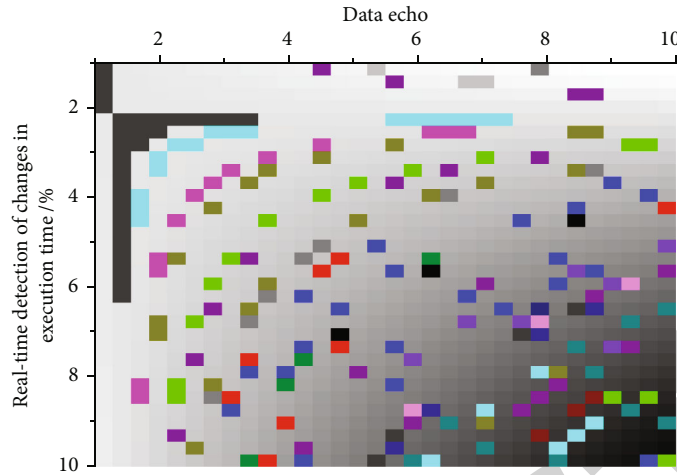


FIGURE 8: Real-time detection of execution time changes.

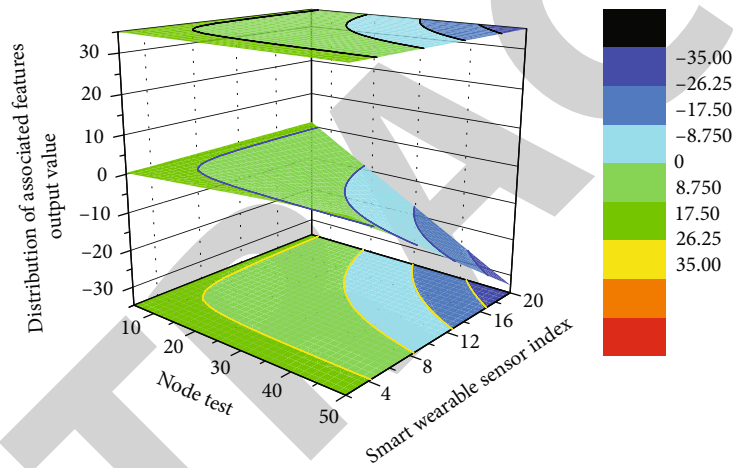


FIGURE 9: Distribution of associated features of smart wearable sensors.

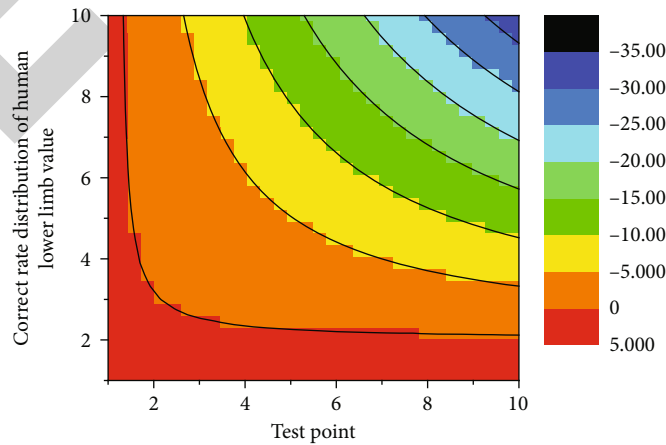


FIGURE 10: Correct rate distribution of human lower limb training recognition algorithm.

whether the human lower limb training recognition model can accurately identify the lower limb training of new users and to examine the problem of user independence. The

ten-fold cross-validation method adopted in subsection, in which the data of the experimenter is also used for experimental training, is highly user-dependent, so a higher

recognition rate can be obtained. But in real life, it makes more sense to study motor lower body training for new users. After referring to a large number of literatures and experimental comparisons, the fuzzy value $b = 2$ set in this paper, the number of clusters of actions $K = 8$, and the set iteration termination threshold $\gamma = 1$. The experiment in this paper can achieve stability after about 14 iterations, and the recognition efficiency is also guaranteed under the condition of ensuring the recognition accuracy.

A total of 8 actions are collected, each action is collected for two minutes, and a total of 400 samples are collected. In this paper, the collected data is windowed in the data pre-processing stage, the window is set to 4 s, and the overlap rate is 50%. This section mainly compares the performance of the HMM and FCM classifiers. The method tested in Figure 10 is to use the self-collected data set collected by a single sensor to compare the accuracy of the two classifiers under the same feature dimension. It can be seen from the identification that the recognition rate of the multifeature fusion algorithm proposed in this paper is higher than 90% in different classifiers, but there are obvious differences between HMM and FCM. HMM needs to learn model parameters from training data, which is a probability model. FCM is a prediction model from data learning, which divides samples into different classes according to similarity or distance, which is a clustering model. The FCM algorithm does not require the parameters of the training model, but only needs to calculate the distance between the test sample and each cluster center, which has the advantage of simplicity and practicality. Traditional machine learning needs to traverse all the data. If there are too many training samples, it will consume a lot of time. The clustering method can reduce the training samples. The more obvious comparison results are shown in the figure. It can be seen from the figure that for this article, the proposed multifeature fusion algorithm, using the unsupervised FCM algorithm, has a significantly higher recognition rate than the HMM algorithm in supervised learning, which strongly proves the advantage of the FCM algorithm based on wearable inertial sensors.

5. Conclusion

This paper builds a self-collected data set to train and test the human lower limb training recognition model proposed in this paper. A large number of experimental results have verified that the classification and recognition accuracy of the hidden Markov model in supervised learning reaches 92.5%, and under the same feature dimension, the recognition efficiency is significantly better than other classical classifiers. The classification method based on fuzzy C-means clustering in unsupervised learning, on the basis of ensuring the recognition rate, has higher execution efficiency and shorter time, and the final recognition rate can reach 95.5%. Finally, a comparative experiment is carried out on the wearing position of the sensor. Aiming at the cloud computing processing of massive lower limb training data, the paper designs a two-dimensional lower limb training recognition depth model based on AlexNet-like model and a one-dimensional lower limb training recognition depth model

based on time series framing network. The deep model of the wearable data is used for lower limb training recognition, and the recognition accuracy of the two models reaches 89.33% and 89.73%, respectively. The research results of this paper further enrich the research on signal perception and abnormal recognition in the field of wearable lower extremity training monitoring and provide new ideas and technical support for wearable lower extremity training signal acquisition and monitoring, early screening of diseases, and intelligent diagnosis and evaluation.

Data Availability

The data used to support the findings of this study are available from the corresponding author upon request.

Conflicts of Interest

The authors declare that they have no known competing financial interests or personal relationships that could have appeared to influence the work reported in this paper.

Acknowledgments

This work was supported by Department of Sports, Henan Institute of Technology.

References

- [1] Q. Zhang, T. Jin, J. Cai et al., "Wearable triboelectric sensors enabled gait analysis and waist motion capture for IoT-based smart healthcare applications," *Advanced Science*, vol. 9, no. 4, p. 2103694, 2022.
- [2] C. Li, Y. He, T. Chen, X. Chen, and S. Tian, "Real-time gait event detection for a lower extremity exoskeleton robot by infrared distance sensors," *IEEE Sensors Journal*, vol. 21, no. 23, pp. 27116–27123, 2021.
- [3] J. Zheng, H. Cao, D. Chen, R. Ansari, K. C. Chu, and M. C. Huang, "Designing deep reinforcement learning systems for musculoskeletal modeling and locomotion analysis using wearable sensor feedback," *IEEE Sensors Journal*, vol. 20, no. 16, pp. 9274–9282, 2020.
- [4] C. Yi, F. Jiang, M. Z. A. Bhuiyan et al., "Smart healthcare-oriented online prediction of lower-limb kinematics and kinetics based on data-driven neural signal decoding," *Future Generation Computer Systems*, vol. 114, pp. 96–105, 2021.
- [5] H. T. T. Vu, D. Dong, H. L. Cao et al., "A review of gait phase detection algorithms for lower limb prostheses," *Sensors*, vol. 20, no. 14, p. 3972, 2020.
- [6] B. Zhang, M. Zhou, and W. Xu, "An adaptive framework of real-time continuous gait phase variable estimation for lower-limb wearable robots," *Robotics and Autonomous Systems*, vol. 143, article 103842, 2021.
- [7] T. Qin, Y. Yang, B. Wen et al., "Research on human gait prediction and recognition algorithm of lower limb-assisted exoskeleton robot," *Intelligent Service Robotics*, vol. 14, no. 3, pp. 445–457, 2021.
- [8] S. Gao, T. He, Z. Zhang, H. Ao, H. Jiang, and C. Lee, "A motion capturing and energy harvesting hybridized lower-limb system for rehabilitation and sports applications," *Advanced Science*, vol. 8, no. 20, p. 2101834, 2021.

- [9] W. Deng, I. Papavasileiou, Z. Qiao, W. Zhang, K. Y. Lam, and S. Han, "Advances in automation technologies for lower extremity neurorehabilitation: a review and future challenges," *IEEE Reviews in Biomedical Engineering*, vol. 11, pp. 289–305, 2018.
- [10] S. Majumder and M. J. Deen, "Wearable IMU-based system for real-time monitoring of lower-limb joints," *IEEE Sensors Journal*, vol. 21, no. 6, pp. 8267–8275, 2021.
- [11] Z. Lv and Y. Li, "Wearable sensors for vital signs measurement: a survey," *Journal of Sensor and Actuator Networks*, vol. 11, no. 1, p. 19, 2022.
- [12] H. Prasanth, M. Caban, U. Keller et al., "Wearable sensor-based real-time gait detection: a systematic review," *Sensors*, vol. 21, no. 8, p. 2727, 2021.
- [13] D. Zeng, C. Qu, T. Ma et al., "Research on a gait detection system and recognition algorithm for lower limb exoskeleton robot," *Journal of the Brazilian Society of Mechanical Sciences and Engineering*, vol. 43, no. 6, pp. 14–15, 2021.
- [14] S. Liu, J. Zhang, Y. Zhang, and R. Zhu, "A wearable motion capture device able to detect dynamic motion of human limbs," *Nature Communications*, vol. 11, no. 1, pp. 11–12, 2020.
- [15] J. Yang, Q. Li, X. Wang et al., "Smart wearable monitoring system based on multi-type sensors for motion recognition," *Smart Materials and Structures*, vol. 30, no. 3, article 035017, 2021.
- [16] I. Sanz-Pena, J. Blanco, and J. H. Kim, "Computer Interface for real-time gait biofeedback using a wearable integrated sensor system for data acquisition," *IEEE Transactions on Human-Machine Systems*, vol. 51, no. 5, pp. 484–493, 2021.
- [17] P. Qin and X. Shi, "Evaluation of feature extraction and classification for lower limb motion based on sEMG signal," *Entropy*, vol. 22, no. 8, p. 852, 2020.
- [18] T. Peng, "A novel motion detecting strategy for rehabilitation in smart home," *Computer Communications*, vol. 150, pp. 687–695, 2020.
- [19] L. Greco, P. Ritrovato, and F. Xhafa, "An edge-stream computing infrastructure for real-time analysis of wearable sensors data," *Future Generation Computer Systems*, vol. 93, pp. 515–528, 2019.
- [20] J. Zhou, S. Yang, and Q. Xue, "Lower limb rehabilitation exoskeleton robot: a review," *Advances in Mechanical Engineering*, vol. 13, no. 4, Article ID 168782, 2021.
- [21] C. F. Chen, H. L. Du ZJ, Y. J. Shi, J. Q. Wang, and W. Dong, "A novel gait pattern recognition method based on LSTM-CNN for lower limb exoskeleton," *Journal of Bionic Engineering*, vol. 18, no. 5, pp. 1059–1072, 2021.
- [22] S. Wu, J. Ou, L. Shu et al., "MhNet: multi-scale spatio-temporal hierarchical network for real-time wearable fall risk assessment of the elderly," *Computers in Biology and Medicine*, vol. 144, article 105355, 2022.
- [23] J. W. Jeong, W. Lee, and Y. J. Kim, "A real-time wearable physiological monitoring system for home-based healthcare applications," *Sensors*, vol. 22, no. 1, p. 104, 2022.